Neurochemistry International 131 (2019) 104546

Contents lists available at ScienceDirect

Neurochemistry International

journal homepage: www.elsevier.com/locate/neuint

Simultaneous quantification of dopamine, serotonin, their metabolites and amino acids by LC-MS/MS in mouse brain following repetitive transcranial magnetic stimulation

Eugenia Z. Poh[a,b,c], Dorothee Hahne[d], Jessica Moretti[a,b,c], Alan R. Harvey[b,c], Michael W. Clarke[d], Jennifer Rodger[a,b,c,*]

[a] School of Biological Sciences, University of Western Australia, 35 Stirling Highway, Crawley, 6009, Western Australia, Australia
[b] School of Human Sciences, University of Western Australia, 35 Stirling Highway, Crawley, 6009, Western Australia, Australia
[c] Perron Institute for Neurological and Translational Science, Australia
[d] Metabolomics Australia, Centre for Microscopy, Characterisation and Analysis, University of Western Australia, 35 Stirling Highway, Crawley, 6009, Western Australia, Australia

ARTICLE INFO

Keywords:
Neurotransmitter
Amino acid
Repetitive transcranial magnetic stimulation
LC-MS/MS

ABSTRACT

Repetitive Transcranial Magnetic Stimulation (rTMS) is a form of non-invasive brain stimulation that has shown therapeutic potential for various nervous system disorders. In addition to its modulatory effects on neuronal excitability, rTMS is capable of altering neurotransmitter (e.g., glutamate, GABA, dopamine and serotonin) concentrations in cortical and subcortical brain regions. Here we used a modified liquid chromatography coupled tandem mass spectrometry (LC-MS/MS) to quantify changes in 27 free amino acids and the monoamines: dopamine (DA), serotonin (5HT) and their metabolites (DOPAC, HVA; 5HIAA) in the mouse brain. Awake C57BL/6 J mice (either sex, 8–12 weeks old) received 10 Hz rTMS using two devices that can deliver low (LI-; 12 mT; custom built) or high (Fo8-; 1.2 T; MagVenture) intensity rTMS. Sham (unstimulated) mice were used as controls. Samples were collected immediately following a single session of rTMS or sham and processed for LC-MS/MS. The modified LC-MS/MS method used to detect DA, 5-HT and their metabolites showed good accuracy and precision with regression coefficients greater than 0.999, and an intra- and inter-day reproducibility with values < 13%. Fo8-rTMS induced a significant reduction in cortical 5-HT turnover rates, hippocampal DOPAC and an increase in striatal DOPAC concentrations. Fo8-rTMS also reduced concentrations of hippocampal α-aminoadipic acid, and striatal serine, threonine, sarcosine, aspartate and glutamate. There were no changes in the level of any compounds following LI-rTMS as compared to sham. The rapid change in monoamine turnover and amino acid concentrations following Fo8-rTMS but not LI-rTMS suggests that different stimulation parameters recruit different cellular mechanisms related to rTMS-induced plasticity. The described method can be used for the characterisation of trace levels of neurotransmitters and amino acids in brain tissue homogenates, providing a useful and precise tool to investigate localised neurotransmitter changes in animal models of health and disease.

1. Introduction

Repetitive Transcranial Magnetic Stimulation (rTMS), a form of non-invasive brain stimulation, has shown therapeutic effects for a range of neurologic and psychiatric disorders (Cirillo et al., 2017), and is approved for use in treatment-resistant depression (Lefaucheur et al., 2014) and more recently, obsessive compulsive disorder (Carmi et al., 2018). Although the mode of action of rTMS remains poorly understood, the procedure has been shown to modulate levels of neurotransmitters, not only within the cortex (Lefaucheur et al., 2014), but also within subcortical regions. Neurotransmitter systems are critical for maintaining homeostatic function of the brain and body. For example, the fine balance between excitatory and inhibitory neurotransmitters, such as glutamate (GLU) and GABA, influence the probability of the brain to undergo synaptic plasticity (Myhrer, 2003). In addition, monoamine neurotransmitters such as dopamine (DA) and

* Corresponding author. School of Biological Sciences M317, University of Western Australia, 35 Stirling Highway, Crawley, 6009, Western Australia, Australia.
E-mail addresses: eugenia.poh@research.uwa.edu.au (E.Z. Poh), dorothee.hahne@gmail.com (D. Hahne), jessica.moretti@research.uwa.edu.au (J. Moretti), alan.harvey@uwa.edu.au (A.R. Harvey), michael.clarke@uwa.edu.au (M.W. Clarke), jennifer.rodger@uwa.edu.au (J. Rodger).

https://doi.org/10.1016/j.neuint.2019.104546
Received 15 February 2019; Received in revised form 7 September 2019; Accepted 8 September 2019
Available online 10 September 2019
0197-0186/

List of abbreviations

Compound

5-HIAA	5-Hydroxyindole-3-acetic acid
5-HT	5-Hydroxytryptamine or serotonin
AAA	α-Aminoadipic acid
ABA	α-Aminobutyric acid
ALA	Alanine
ARG	Arginine
ASN	Asparagine
ASP	Aspartic acid/Aspartate
C–C	Cystine
CIT	Citrulline
CTH	Cystathionine
d3MET	d3-Methionine
DA	Dopamine
DOPAC	3,4-Dihydroxyphenylacetic acid
GABA	γ-Amino-n-butyric acid
GLN	Glutamine
GLU	Glutamic acid/Glutamate
GLY	Glycine
HARG	Homoarginine
HIS	Histidine
HLY	Hydroxylysine (2 isomers)
HPHE	Homophenylalanine
HVA	Homovanillic acid
ILE	Isoleucine
LEU	Leucine
LYS	Lysine
MET	Methionine
ORN	Ornithine
PHP	Proline-hydroxyproline (dipeptide)
PRO	Proline
SAR	Sarcosine
SER	Serine
ß-AIB	ß-Aminoisobutyric acid
THR	Threonine
TRP	Tryptophan
TYR	Tyrosine
VAL	Valine

Other

ANOVA	Analysis of variance
Fo8-rTMS	repetitive Transcranial Magnetic Stimulation using a commercially available high intensity figure-of-eight coil
LI-rTMS	repetitive Transcranial Magnetic Stimulation using a custom built low-intensity miniaturised circular coil
LC	Liquid chromatography
-MS/MS	- coupled tandem mass spectrometry
MRM	Multiple reaction monitoring
MRS	Magnetic resonance spectroscopy
MS	Mass spectrometry
NT	Neurotransmitters
rTMS	repetitive Transcranial Magnetic Stimulation
SEM	Standard error of the mean

serotonin (5-hydroxytryptamine; 5-HT) are implicated in the pathophysiology of various neuropsychiatric disorders including schizophrenia, depression and drug addiction (Grace, 2004; Thomas et al., 2008; Winograd-Gurvich et al., 2006). Therefore, alterations to neurotransmitter imbalances within the brain by therapeutic interventions such as rTMS are a likely mechanism contributing to the beneficial effect of rTMS therapy and there is a need to better understand these alterations in order to optimise therapeutic interventions.

Characterisation of neurotransmitters in the human brain following rTMS has been carried out using non-invasive imaging techniques such as MRS and PET scans. rTMS targeted to the human motor cortex has been shown to induce striatal DA release, likely due to activation of corticofugal projections (Strafella et al., 2003, 2001). In addition, a single session of rTMS has been shown to increase levels of combined GLU and glutamine, a GLU metabolite, in the dorsolateral prefrontal cortex (Michael et al., 2003). However these non-invasive imaging methods are currently unable to simultaneously detect a wide range of compounds within the brain (Badgaiyan, 2014) or to quantify those at extremely low concentrations (Verma et al., 2016). By contrast, invasive sampling techniques provide researchers with the opportunity to use sophisticated chemical analytical methods such as liquid chromatography coupled tandem mass spectrometry (LC-MS/MS) to detect a broad range of target compounds with high sensitivity and specificity. LC-MS/MS systems are able to simultaneously identify and quantify various neurotransmitters, their metabolites and free-form amino acids (AAs) in complex mixtures at *picomolar* concentrations (Ewles and Goodwin, 2011).

Murine models used to investigate the neurochemical changes induced by a single session of rTMS have shown altered concentrations of DA, 5-HT and their metabolites DOPAC, HVA and 5-HIAA in the cortical regions such as the prefrontal cortex, hippocampus and dorsal/ventral striatum (Ben-Shachar et al., 1997; Kanno et al., 2004; Keck et al., 2002; Zangen and Hyodo, 2002), as well as increased of GLU concentrations in the ventral striatum (Zangen and Hyodo, 2002). However, most studies of rTMS effects on rodent brain chemistry have used commercially available rodent coils, or small human coils, which are relatively large compared to the subject's head, raising concerns about the focality of stimulation and relevance to human studies (Rodger and Sherrard, 2015; Vahabzadeh-Hagh et al., 2012). Use of these commercially available coils result in widespread stimulation of the rodent's head and/or body (Rodger and Sherrard, 2015). Our lab has therefore developed miniature coils that target small areas of the brain in murine models, more closely replicating focal stimulation in humans, albeit at a lower magnetic field intensity (Rodger and Sherrard, 2015; Tang et al., 2015) than those routinely used in human studies (i.e., high intensity rTMS). We have previously shown that a single session of low intensity rTMS *in vitro* alters neuronal excitability (Tang et al., 2016) and cellular metabolites related to the Kreb's cycle (Hong et al., 2018), and improves abnormal visual circuits following 14 days of treatment *in vivo* (Makowiecki et al., 2014; Poh et al., 2018; Rodger et al., 2012). However, changes to neurotransmitters and cellular metabolites following a single session of low intensity rTMS have not been assessed *in vivo*. Because this is the first study to simultaneously quantify a large number of neurotransmitters and amino acids *in vivo* in the context of rTMS, it was also of interest to compare the effects of our rodent-specific coil to those of a commercially available figure-of-eight rTMS coil (MagVenture, Denmark) that has been used to deliver high intensity rTMS in human trials (Hilbert et al., 2019; Zimmermann et al., 2016).

The aims of the present study were to i) develop a method using LC-MS/MS to accurately and simultaneously quantify the concentrations of DA, 5-HT and their metabolites (DOPAC, HVA; 5-HIAA) in samples from mouse brain, ii) combine this method with a commercially available sample preparation kit designed to detect and quantify up to 33 amino acids simultaneously, and iii) use this method to investigate the effects of our custom made circular low intensity rTMS coil (LI-rTMS) and a commercially available high intensity figure-of-eight coil (Fo8-rTMS) against control animals on neurotransmitter and metabolite

concentrations in the mouse cortex, hippocampus and striatum.

2. Materials and methods

2.1. LC-MS/MS conditions

The method described below was developed by us to optimise simultaneous detection of DA, 5HT and their metabolites using the previous study by Kim et al. (2016) as a starting point for LC-MS/MS conditions.

2.1.1. DA, 5-HT and their metabolites

Analysis was conducted using an Agilent 6460 LC-MS instrument operated in 2D mode. With the addition of a second-dimension, the resolution and sensitivity of LC-MS/MS produced chromatograms can be further enhanced in targeted analysis of complex mixtures through the use of two separation columns (i.e., in 2D-LC mode) (Leonhardt et al., 2015). The first-dimension column was an Agilent Poroshell EC120 2.1 × 50 mm x 2.7 µm C18 column; and the second-dimension a Phenomenex 3 × 150 mm × 2.6 µm Biphenyl column (Torrance, USA). LC-MS grade solvents were 0.1% formic acid in water (A) and 0.1% formic acid in methanol (B). Initial conditions were 98% A, 2% B. Compounds were eluted by increasing to 98% B over 5 min, and the columns re-equilibrated for 3 min prior to the next injection. Compounds assayed were heart cut from column 1 to column 2 between 0.3 and 3.9 min.

2.1.2. Derivatised free amino acids

A single EZ:faast AAA-MS column 250 × 2.0 mm was used on the Agilent 6460 LC-MS instrument. The mobile phase and elution gradient were done as described in the EZ:faast kit manual. LC-MS grade solvents were 10 mM Ammonium formate in water (A) and 10 mM Ammonium formate in methanol (B). Initial conditions were 68% B, 32% A, increasing to 83% B over 13 min, then returning to 68% B over the next 4 min.

2.1.3. Data collection

Target compound multiple reaction monitoring (MRM) transition, shown as precursor and product ion mass to charge ratio (m/z), retention time, collision energy used and ionization polarity for DA/5-HT and derivatised amino acids are shown in Tables 1 and 2, respectively. Chromatogram peaks were integrated and quantified using the MassHunter Quantitative Analysis software (Agilent Technologies, Santa Clara, United States; Fig. 1). Data was collected from compounds with a signal to noise (S/N) ratio > 10. However, compounds with a S/N > 7 and an obvious chromatogram peak were also included following manual inspection.

2.2. Materials

LC-MS grade dopamine hydrochloride (DA), 3,4-dihydroxyphenylacetic acid (DOPAC), homovanillic acid (HVA), serotonin (5-HT) and 5-hydroxyindole-3-acetic acid (5-HIAA) were purchased from Sigma-Aldrich (St. Louis, MO, USA). DA-d_4, DOPAC-$^{13}C_3$, HVA-d_3, 5-HT-d_4 and 5-HIAA-$^{13}C_3$ were purchased from Toronto Research Chemicals (Toronto, ON, Canada). The working standard (DA, 0.61 ng/mL; DOPAC, 7.05 ng/mL; HVA, 7.29 ng/mL; 5-HT, 35.2 ng/mL and 5-HIAA, 0.76 ng/mL) and working internal standard solutions (DA-d_4, 50 ng/mL; DOPAC-$^{13}C_3$, 50 ng/mL; HVA-d_3, 500 ng/mL; 5-HT-d_4, 50 ng/mL; and 5-HIAA-$^{13}C_3$, 500 ng/mL) were diluted in dH_2O (LC-MS grade). Reagents used for the simultaneous quantification of the 33 free amino acids were completed using the commercially available EZ:Faast kit (Phenomenex, Torrance, USA). Calibration curves were prepared by serial dilution of the working standards (Fig. 2). ARG was standardised against the d3MET IS as the regression coefficients of the calibration curve was larger when compared to standardisation against the recommended HARG IS.

2.3. Animals

All experiments were performed in accordance with the National Health and Medical Research guidelines and approved by The University of Western Australia Animal Ethics Committee (AEC 100/1453). Wildtype (C57BL/6 J) mice (sham: F = 2, M = 3; LI-rTMS: F = 2, M = 3, Fo8-rTMS: F = 3, M = 3) were sourced from the Animal Resources Centre (Canning Vale, Australia). Fisher's exact test showed no significant differences between stimulation groups in the frequency of gender ($p > 0.99$). All animals were of adult age during experimental testing (8–12 weeks) and housed in 12 h light/dark cycle with food and water provided *ad libitum*. Grids were removed from cages of animals that underwent coil support surgeries (as described in Poh et al., 2018) and were given hydrogel (Necta H2O, Able Scientific, Australia) as a water substitute.

2.4. Magnetic stimulation

Mice were gender matched and allocated to one of three groups: sham, LI-rTMS or Fo8-rTMS. Each mouse received a single stimulation session at 10 Hz and stimulation parameters are described below.

For sham (handling controls) and LI-rTMS animals, a coil support

Table 1
Optimal conditions of LC-MS/MS used for the quantification of DA, 5-HT and their metabolites (and labelled versions) in mouse brain homogenates.

Compound name	Precursor ion (m/z)	Product ion (m/z)	Retention time (min)	Collision Energy (V)	Ionization polarity
DA	154.1	137.1	2.95	15	Positive
DA-d_4	158.1	141.1[a]	2.99	15	Positive
		95			
DOPAC	167.1	123.1	4.90	2	Negative
DOPAC-d_5	172.1	123.1	4.90	5	Negative
HVA	181.2	137.2	5.30	15	Negative
HVA-d_3	184.2	140.1[a]	5.80	2	Negative
		122.1			
5-HT	177.2	160.2	4.44	16	Positive
5-HT-d_4	181.2	164.1[a]	4.43	15	Positive
		136.1			
5-HIAA	192.2	146.2	5.15	16	Positive
5-HIAA-$^{13}C_3$	197.2	150[a]	5.15	15	Positive
		123			

[a] Transitions used for quantification.

Table 2
Optimal transitions used for the quantification of derivatised amino acids (as shown by the precursor ion charge) using the EZ:faast kit.

	Compound name	Precursor ion (*m/z*)	Product ion (*m/z*)	Retention time (min)	Collision Energy (V)	IS used for quant.	Lowest conc. quantified (pM)
Essential AAs	HIS	370.2	196.3	6.123	33	d3MET	8.734
	ILE	260.3	172.1	7.834	17	d3MET	349.3
	LYS	361.2	301.3	5.932	20	d3MET	912.2
	LEU	260.3	172.1	7.460	17	HPHE	107.4
	PHE	294.3	206.1	7.563	17	HPHE	1.494
	MET	278.3	190.1	5.603	17	d3MET	175.6
	TRP	333.3	245.1	6.630	21	d3MET	1.938
	THR	248.3	160.2	3.800	10	d3MET	0.594
	VAL	246.3	158.1	6.417	17	d3MET	341.6
Non-essential AAs	ALA	218.3	130.1	4.421	13	HPHE	289.1
	ASN	243.0	157.2	3.803	5	d3MET	38.80
	ASP	304.3	216.2	6.032	19	d3MET	517.1
	ARG	303.4	69.9	2.560	51	d3MET	962.74
	C–C	497.2	248.2	8.616	25	HPHE	7.949
	GABA	232.0	172.0	4.718	13	d3MET	5.253
	GLN	275.3	172.1	3.143	21	d3MET	3784
	GLU	318.3	172.1	6.365	21	d3MET	6820
	GLY	204.4	144.0	3.807	5	d3MET	459.8
	SER	234.3	146.0	3.398	15	d3MET	1036
	PRO	244.3	156.2	5.879	20	d3MET	30.12
	TYR	396.2	136.2	9.313	43	HPHE	56.50
Other AA	AAA	332.3	244.2	7.092	19	HPHE	0.912
	ABA	232.0	172.0	6.343	13	d3MET	1456
	ß-AIBA	232.0	172.0	5.045	13	d3MET	3057
	CIT	304.3	156.3	3.212	25	HARG	937.8
	CTH	479.3	230.1	8.500	23	HPHE	231.0
	SAR	218.0	88.0	4.960	20	d3MET	740.1
IS	HARG	371.3	84.1	3.056	53	–	
	d3MET	281.3	193.1	5.564	17	–	
	HPHE	308.3	220.2	8.750	15	–	

AA = amino acid, IS = internal standards.

was attached to the surface of the skull (Poh et al., 2018) and mice were allowed to recover for one week. Briefly, animals were anaesthetised and the skin was cut to expose the skull. A plastic support was attached to the surface of the skull above lambda using cyanoacrylate and dental cement. The skull was not penetrated and the brain not exposed during surgery. *Post hoc* immunofluorescent staining for microglia and activated astrocytes did not reveal any differences in the motor, somatosensory and visual cortex between animals that underwent surgery and control animals (Supplementary Figure 1), suggesting that attachment of the coil support did not affect the brain itself. Thus, sham animals with no active stimulation were used as handling controls for both stimulation groups (LI- and Fo8-rTMS).

The coil support allowed consistent positioning of the small coils in awake and freely moving mice, maximising reproducibility and minimising stress to the mice (Poh et al., 2018). The custom-made coil comprised of 300 windings of copper wire (0.125 mm in diameter) with an inner and outer diameter of 6 and 8 mm, respectively, connected to an electromagnetic pulse generator (e-cell^{TM}) programmed to deliver LI-rTMS at 10 Hz for 10 min. It has been shown previously that the temperature of the custom-made coil does not go above 37 °C and it's vibration is within the amplitude range of background, when stimulated using the 10 Hz protocol, thus ruling out potential heating effect on the brain (Grehl et al., 2015). Maximum field intensity at the base of the coil was 12 mT. Sham animals had the coil attached to the support for 10 min, but with the device switched off.

In the third group, rTMS was delivered using the commercially available high intensity figure-of-eight coil (Fo8-rTMS, MC-B65-HO, MagVenture, Denmark). Because of its large size and weight, it was not possible to attach the coil to a support on the mouse head. Instead, mice were habituated to handling and presence of the coil above the head for one week prior to stimulation, allowing Fo8-rTMS to be delivered to lightly restrained, awake mice. We applied Fo8-rTMS at 20% maximum stimulator output (MSO; approximating mouse motor threshold), which corresponds to approximately 1.2 T, at a frequency of 10 Hz. Due to heating of the coil (> 40 °C), only 6 min of stimulation could be applied (3600 pulses) to the Fo8-rTMS group.

2.5. Sample preparation

Immediately after stimulation, mice were terminally anaesthetised using sodium pentobarbitone (0.1 mL, i.p.; Lethabarb, Virbac, Australia) and decapitated. The cortex, hippocampus and striatum from both hemispheres were immediately dissected on ice, rapidly frozen with liquid nitrogen and homogenised using a tissue pulveriser cooled with dry ice. Homogenates were stored at −80 °C until analysis. Prior to the first injection into the LC-MS/MS instrument, 300 µL of ice-cold 0.2 M perchloric acid was added to each tube, vortexed for 5 s and centrifuged for 15 min at 15 000 rpm at 4 °C. For the DA/5-HT analysis, 100 µL of the supernatant and 50 µL of the working internal standard solution (see 3.4 Materials) were transferred into autosampler vials for direct sampling in the LC-MS/MS instrument. Preliminary analyses determined that the concentration of some amino acids, e.g. GLU, in 100 µL of supernatant exceeded the maximal recommended calibration point concentration (200 µM). Therefore, samples were diluted by a factor of 10, i.e. 10 µL of supernatant added to 90 µL of 0.2 M perchloric acid. Samples and calibration solutions were cleaned up and derivatised as instructed in the EZ:faast user guide (Phenomenex, Torrance, USA). Remaining supernatants were stored at −80 °C.

2.6. Assay validation

Calibration standards were prepared by serially diluting from a stock solution. Quality controls (QCs) for the DA/5-HT were from a separate whole mouse brain homogenate, prepared as described in Section 3.5, but suspended in 1450 µL of ice-cold 0.2 M perchloric acid. As the EZ:Faast kit is commercially available, we only assessed the intra- (within-run precision) assay variability. The QC samples were derived from the supernatant of one brain sample assayed three times.

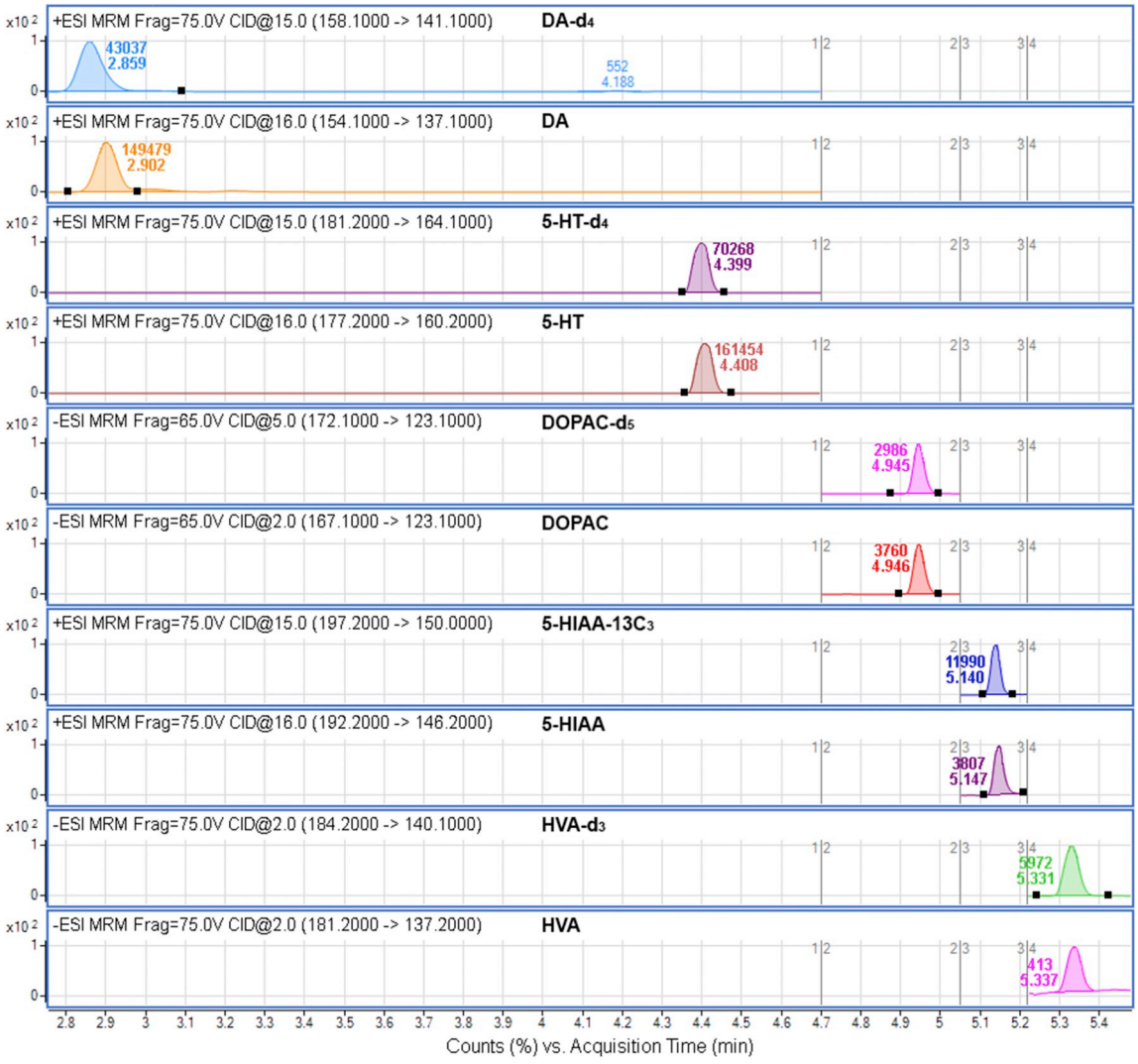

Fig. 1. Example chromatogram of DA, 5-HT, their metabolites and labelled versions from a mouse whole-brain homogenate. A whole-brain homogenate was used as the quality control to develop inter- and intra-assay coefficients of variation (%CV).

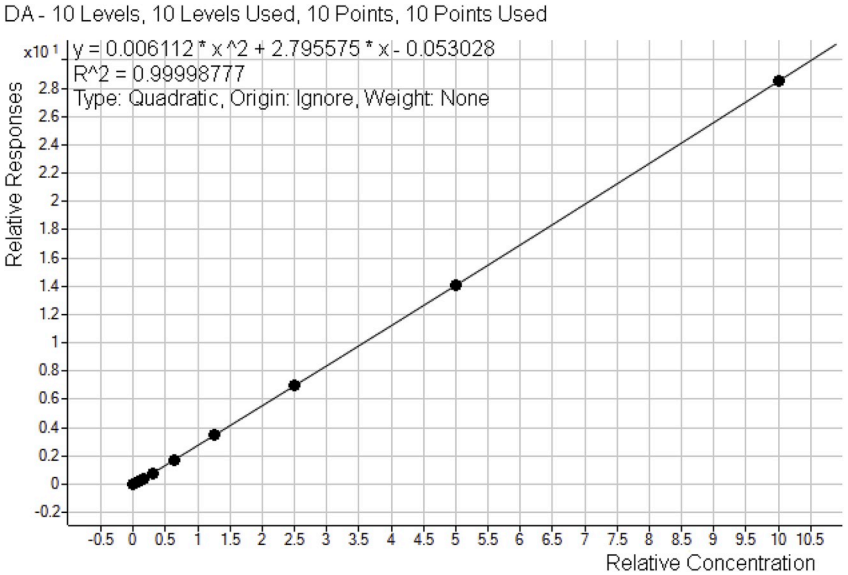

Fig. 2. Standard curve used for DA quantification, $r^2 = 0.99999$. X-axis is concentration (μM) and Y-axis if for relative response of DA corrected by its internal standard (DA-d_4). Additional calibration curves can be found in the Supplementary Section Fig. 2.

After addition of 300 µL of ice-cold 0.2 M perchloric acid, the supernatant was diluted by a factor of 20, derivatised and assayed as per manufacturer's instructions (Phenomenex, Torrance, USA).

2.7. Statistical analyses

Raw data were processed using Microsoft Excel and values reported for the two methods normalised to original dissected tissue mass (mg). SPSS (version 24.00, IBM) was used for statistical analyses and significance set at the level of $p < 0.05$. Figures were created using Prism 7 (GraphPad Software). Because two different LC-MS/MS assays were used, statistical analyses were separated into i) DA, 5-HT and their metabolites and ii) free amino acids. Changes in compound concentrations (pmol/mg) and turnover rates for each brain region (cortex, hippocampus and striatum) were performed using Welch's ANOVAs and *post hoc* Games-Howell test. Quantitative data for each method were calculated as mean ± SEM for each group (stimulation x brain region).

DA and 5-HT turnover rates were then calculated by summing the final concentration of each metabolite and dividing by the parent compound:

$$\frac{[DOPAC] + [HVA]}{[DA]} \; ; \; \frac{[5 - HIAA]}{[5 - HT]}$$

This index estimates the accumulation of a particular neurotransmitter relative to its metabolite(s). An increase in the index suggests more of the neurotransmitter being broken down, resulting in a decreased probability for the compound to bind to a postsynaptic site and exert its effect. Because the index is a measure of proportional data, the non-parametric Kruskal-Wallis tests were used to compare rank differences in DA and 5-HT turnover rates between stimulation groups. Where appropriate, *post hoc* Mann-Whitney U tests with Bonferroni corrections were applied.

3. Results

3.1. DA, 5-HT and their metabolites

3.1.1. Method optimisation

Preliminary assessment of tissue samples extracted in 0.1% formic acid showed a 10–50% recovery rate of the target compounds compared to 0.2 M perchloric acid (data not shown). Therefore, all subsequent supernatants were prepared by homogenising samples in 0.2 M perchloric acid and spiked with the working internal standards.

3.1.2. Precision and accuracy

QC samples were assayed to produce an intra- (within-run precision) and inter- (between-run precision) assay coefficient of variation (CV%). All values were < 13%, indicating repeatability and reliability of the present method, with no significant deviations in precision between and within runs (see Table 3).

3.1.3. Effect of magnetic stimulation

In the cortex, neither LI- nor Fo8-rTMS affected compound concentrations of DA ($F_{(2,\ 5.75)} = 1.69$, $p = 0.264$), DOPAC ($F_{(2,\ 6.46)} = 1.04$, $p = 0.403$), HVA ($F_{(2,\ 2.43)} = 3.08$, $p = 0.215$), 5-HT ($F_{(2,\ 7.16)} = 1.98$, $p = 0.206$) and 5-HIAA ($F_{(2,\ 6.79)} = 0.41$, $p = 0.676$; Fig. 3). We did not observe a difference in DA turnover rates ($H(2) = 1.220$, $p = 0.543$), but a trend to significance for 5-HT turnover rates ($H(2) = 5.460$, $p = 0.065$). We conducted follow-up tests despite the non-significant finding for 5-HT turnover rates because it has been shown that this index is altered in patients with depression (Barton et al., 2008), which may be a mechanism of the beneficial effects of rTMS in patients. Follow-up Mann-Whitney tests with Bonferroni correction (i.e., at a 0.0167 level of significance, two tailed) showed that Fo8-rTMS (*Mean rank* = 3.00) significantly reduced 5-HT turnover rates when compared to sham (*Mean rank* = 8.00; $U = 0$, $p = 0.009$), but not LI-rTMS (*Mean rank* = 4.60) compared to sham groups (*Mean rank* = 6.40; $U = 8$, $p = 0.347$; Table 4). This finding indicates a proportional increase in 5-HT concentrations within the cortex, and/or a decrease in its metabolite concentration, 5-HIAA, following Fo8-rTMS.

In the hippocampus, analysis of HVA concentrations was not carried out due to low concentrations and poor S/N ratios (refer to section 2.1.3). We observed a significant effect of stimulation on DOPAC concentrations ($F_{(2,\ 7.52)} = 6.45$, $p = 0.023$) and a trend towards significance for DA ($F_{(2,\ 7.49)} = 4.24$, $p = 0.059$) but no effect on 5-HT ($F_{(2,\ 8.15)} = 0.21$, $p = 0.811$) and 5-HIAA concentrations ($F_{(2,\ 7.5)} = 0.67$, $p = 0.538$; Fig. 3). *Post hoc* tests for DOPAC concentrations revealed a significant difference between LI-rTMS and Fo8-rTMS ($p = 0.036$), and a trend towards significance between sham and Fo8-rTMS ($p = 0.084$). There were no significant differences detected between all stimulation groups for DA ($H(2) = 1.112$, $p = 0.574$) and 5-HT ($H(2) = 0.193$, $p = 0.908$) turnover rates (Table 4). Thus, our results show that Fo8-rTMS reduces the concentration of DOPAC, a DA metabolite, but not DA itself.

Lastly, there was a significant effect of stimulation on DOPAC concentrations in the striatum ($F_{(2,\ 6.99)} = 4.93$, $p = 0.045$) but not for any other compound (DA: $F_{(2,\ 7.06)} = 0.64$, $p = 0.550$; HVA: $F_{(2,\ 8.19)} = 2.74$, $p = 0.122$; 5-HT: $F_{(2,\ 6.4)} = 1.26$, $p = 0.343$; 5-HIAA: $F_{(2,\ 8.65)} = 1.22$, $p = 0.339$; Fig. 3). *Post hoc* tests revealed no significant differences between stimulation groups in DOPAC concentrations, although there was a trend to significance between sham and LI-rTMS animals ($p = 0.059$). There were also no significant differences detected in turnover rates in the striatum for DA ($H(2) = 2.028$, $p = 0.363$) or 5-HT ($H(2) = 3.841$, $p = 0.147$; Table 4).

3.2. Derivatised amino acids

Preliminary analysis deemed the concentrations of certain target molecules too concentrated for analysis. Therefore, following homogenisation in perchloric acid, supernatants were further diluted by a factor of 10 in 0.2 M perchloric acid (10 µL supernatant + 90 µL acid) and samples derivatised as per the manufacturer's instructions (Phenomenex, Torrance, USA).

3.2.1. Precision and accuracy

The intra-assay CV% could not be determined for LYS, CTH and CIT, due to the low S/N ratios recorded in the QC samples. For all other compounds, with the exception of ARG (27.75%), intra-assay CV%

Table 3
Precision of QC samples for the assessment of DA, 5-HT and their metabolites.

Compound name	Individual (CV%)	Repeatability (intra-assay) (CV%)	Intermediate precision (inter-assay) (CV%)
DA	10.86, 2.50, 4.80	6.05	3.18
DOPAC	11.01, 15.82, 11.12	12.65	10.27
HVA	13.49, 3.38, 2.26	6.37	7.86
5-HT	19.56, 7.40, 2.43	9.80	12.48
5-HIAA	20.51, 12.55, 5.18	12.75	2.19

CV = coefficient of variation.

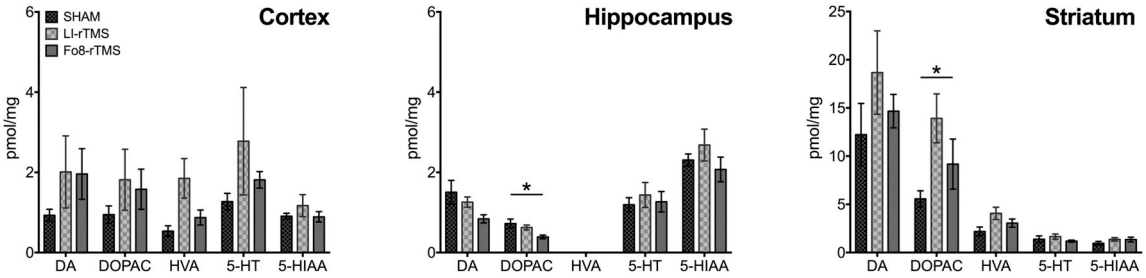

Fig. 3. DA, 5-HT and their metabolite concentrations (pmol/mg) following sham, a single session of low intensity (LI-) and high intensity figure-of-eight (Fo8-) rTMS in adult mice. Welch's ANOVA showed a significant effect of stimulation on DOPAC concentrations in the hippocampus ($p = 0.023$) and striatum ($p = 0.046$). *$p < 0.05$. Reported values are means ± SEM.

were < 20%: essential AAs: HIS (3.76%), ILE (2.66%), LEU (3.85%), PHE (1.03%), MET (3.25%), TRP (0.58%), THR (7.62%), VAL (3.67%); non-essential AAs: ALA (2.29%), ASN (6.4%), ASP (14.1%), C–C (1.03%), GABA (18.71%), GLN (3.07%), GLU (7.27%), GLY (4.88%), SER (3.58%), PRO (3.67%), TYR (2.19%), and other AAs: AAA (3.24%), ß-AIBA (12.08%), SAR (2.26%), indicating good precision and accuracy of the current method.

3.2.2. Effect of magnetic stimulation

The amino acids 1-methyl-histidine, α-aminopimelic acid, DA, glycine-proline (dipeptide), hydroxylysine4-hydroxyproline, phenylalanine, thiaproline were unable to be detected in the diluted supernatant of all homogenised brain regions and were therefore excluded from further analysis (refer to section 2.1.3).

Within cortical and hippocampal brain regions, there were no significant differences in amino acid levels between sham, LI- and Fo8-rTMS groups, with the exception of α-aminoadipic acid concentration in the hippocampus ($F_{(2,6.48)} = 6.54$, $p = 0.028$; Table 5). Changes to striatal concentrations were observed for serine ($F_{(2,7.2)} = 5.012$, $p = 0.043$), threonine ($F_{(2,7.3)} = 9.237$, $p = 0.01$), sarcosine ($F_{(2,4.74)} = 18.784$, $p = 0.006$), aspartate ($F_{(2,6.56)} = 11.54$, $p = 0.007$) and GLU ($F_{(2,5.76)} = 13.78$, $p = 0.006$) concentrations (Table 5). *Post hoc* Games-Howell tests revealed no significant differences between sham and LI-rTMS groups. Comparisons were therefore made against Fo8-rTMS. All tests showed a reduction in concentrations following Fo8-rTMS: α-aminoadipic acid (sham $p = 0.054$; LI-rTMS $p = 0.023$), threonine (sham $p = 0.020$; LI-rTMS $p = 0.021$), aspartate (sham $p = 0.010$; LI-rTMS $p = 0.020$), GLU (sham $p = 0.012$; LI-rTMS $p = 0.013$), serine (sham $p = 0.067$; LI-rTMS $p = 0.098$) and sarcosine (sham $p = 0.005$; LI-rTMS $p = 0.287$; Table 5).

4. Discussion

In the present study, we sought to investigate the effects of a single LI- or Fo8-rTMS stimulation on various neurotransmitter and amino acid concentrations and developed a method to identify and quantify simultaneously DA, 5-HT and their metabolites (DOPAC, HVA; 5-HIAA) and 33 free amino acids from mouse brain. Our findings show significant changes in 5-HT turnover in the cortex following Fo8-rTMS and altered DOPAC concentrations in the hippocampus and striatum. Twenty-seven free AAs were quantifiable using our technique, and we found a significant reduction of α-aminoadipic acid concentrations in the hippocampus and a reduction of serine, threonine, sarcosine, aspartate and GLU concentrations in the striatum following Fo8-rTMS, but not LI-rTMS, compared to sham stimulated animals.

4.1. Effect of the present high intensity Fo8-rTMS protocol

4.1.1. Dopamine and serotonin changes

We observed a reduction in 5-HT turnover rates in the cortex following high intensity Fo8-rTMS, indicating a *relative* increase in 5-HT concentration and reduced concentration of its metabolite, 5-HIAA. Similarly, within the hippocampus and striatum, there were changes in DOPAC concentrations, a metabolite of DA. Our results suggest that the present Fo8-rTMS protocol may acutely influence the activity of enzymes related to the metabolism of 5-HT to 5-HIAA (monoamine oxidase) and of DA to DOPAC (monoamine oxidases, aldehyde dehydrogenase and catechol-O-methyl transferase (Meiser et al., 2013)).

Our findings for 5-HT are consistent with the lack of change in 5-HT levels only in rats following rTMS (Ben-Shachar et al., 1997) and in olfactory bulbectomy mice following rTMS delivered using a high intensity circular coil (Heath et al., 2018). It is possible that the rTMS-induced reduction in 5-HT metabolism may underpin its therapeutic effects in patients with Major Depression Disorder (MDD; Lefaucheur et al., 2014; O'Reardon et al., 2007a, 2007b), because un-medicated patients diagnosed with MDD have elevated 5-HT turnover rates (Barton et al., 2008). However, the lack of change observed for DA concentrations differs from previous studies showing an increase in DA following various high intensity rTMS protocols. In rats, two studies have demonstrated increased DA in the frontal cortex, hippocampus and striatum following rTMS (Ben-Shachar et al., 1997; Keck et al., 2002). Similar to the present sampling methods of this study, previously, brain homogenates were analysed by HPLC immediately following a single stimulation session, thus detecting all DA present within cells and in the extracellular space (Ben-Shachar et al., 1997). In contrast, Keck et al. (2002) used microdialysis, which is method considered to sample only from the extracellular space, over a period of several hours following a single stimulation. The results from the two studies differ in that the first study (Ben-Shachar et al., 1997) found immediate changes in the frontal cortex, hippocampus and striatum post-

Table 4
DA and 5-HT turnover rates (mean ± SEM) in various brain regions following LI- and Fo8-rTMS.

	Cortex			Hippocampus			Striatum		
	Sham	LI-rTMS	Fo8-rTMS	Sham	LI-rTMS	Fo8-rTMS	Sham	LI-rTMS	Fo8-rTMS
DA	1.283 ± 0.173	1.100 ± 0.167	1.326 ± 0.060	0.492 ± 0.031	0.502 ± 0.033	0.472 ± 0.045	0.746 ± 0.147	1.040 ± 0.158	0.796 ± 0.115
5-HT	0.775 ± 0.097	0.575 ± 0.116	**0.497 ± 0.054	2.039 ± 0.196	2.074 ± 0.381	1.803 ± 0.311	0.749 ± 0.079	0.853 ± 0.075	1.123 ± 0.150

**$p = 0.009$ vs. sham; based on Mann-Whitney U tests on rank differences with Bonferroni correction.

Table 5
Concentration (mean ± SEM nmol/mg of wet tissue mass) of various amino acids as determined by using the EZ:faast kit in mouse brain homogenates.

		Cortex				Hippocampus
		Sham	LI-rTMS	Fo8-rTMS	F, *p*	Sham
Essential AA	HIS	90.5 ± 25.19	118.26 ± 49.13	107.49 ± 32.43	0.153, 0.86	144.51 ± 102.89
	ILE	121.92 ± 13.25	138.83 ± 17.55	119.18 ± 12.32	0.396, 0.691	224.18 ± 19.91
	LYS	337 ± 29.24	502.52 ± 84.35	400.11 ± 30.05	2.142, 0.185	551.41 ± 12.92
	LEU	109.14 ± 14.05	136.86 ± 25.83	101.53 ± 7.91	0.817, 0.481	120.31 ± 20.95
	PHE	73.8 ± 6.8	106.27 ± 22.73	83.51 ± 18.91	0.903, 0.452	104.44 ± 65.75
	MET	91.5 ± 7.85	99.63 ± 13.43	86.78 ± 10.8	0.256, 0.781	336.39 ± 195.42
	TRP	23.19 ± 3.58	32.63 ± 8.5	18.62 ± 4.03	1.088, 0.385	20.75 ± 11.81
	THR	364.9 ± 30.42	540.88 ± 113.59	310.74 ± 28.09	2.23, 0.176	254.98 ± 90.19
	VAL	197.04 ± 21.16	209.05 ± 27.23	180.65 ± 21.97	0.321, 0.735	359.48 ± 56.43
Non-essential AA	ALA	1509.01 ± 156.02	2002.61 ± 408.66	1495.27 ± 133.72	0.652, 0.549	1864.95 ± 185.52
	ASN	40.56 ± 11.74	383.67 ± 334.15	74.3 ± 14.81	1.821, 0.26	
	ASP	10296.6 ± 802.55	13959.25 ± 2198.3	9814.97 ± 560.4	1.55, 0.277	4011.91 ± 1157.9
	ARG	390.67 ± 51.32	484.86 ± 57.46	390.66 ± 20.63	1.098, 0.388	937.85 ± 251.7
	C–C	50.36 ± 3.31	60.76 ± 12.05	44.16 ± 6.45	0.736, 0.514	87.06 ± 80.04
	GABA	6732.55 ± 709.43	9403.09 ± 1781.12	7799.38 ± 646.58	1.154, 0.366	5995.28 ± 1605.12
	GLN	9969.72 ± 445.36	13913.33 ± 2382.37	12338.54 ± 1519.56	2.088, 0.206	7279.62 ± 1195.34
	GLU	21607.05 ± 1451.47	29363.83 ± 4675.05	23285.08 ± 1487.4	1.261, 0.338	16212.93 ± 2786.81
	GLY	2829.88 ± 322.82	3671.68 ± 689.94	2743.97 ± 147.49	0.79, 0.493	1929.01 ± 426.04
	SER	1405.9 ± 131.98	1733.96 ± 364.37	1376.34 ± 62.22	0.432, 0.667	1054.71 ± 194.69
	PRO	233.07 ± 29.82	284.29 ± 45.66	234.47 ± 23.3	0.482, 0.636	118.85 ± 40.64
	TYR	37.95 ± 6.71	59.47 ± 13.9	59.65 ± 24.39	1.105, 0.386	157.1
Other AA	AAA	99.72 ± 6.5	133.16 ± 28.74	86.83 ± 19.59	0.804, 0.49	96.13 ± 8.92
	ABA	2332.46 ± 242.55	3219.93 ± 595.55	2669.46 ± 228.42	1.072, 0.39	2383.57 ± 559.87
	ß-AIBA	2333.2 ± 242.6	3221.49 ± 595.9	2670.23 ± 228.2	1.073, 0.39	2616.8 ± 403.97
	CIT	359.14 ± 40.41	345.09 ± 31.21	240.96 ± 32.41	3.357, 0.088	799.94 ± 137.69
	CTH	48.5 ± 3.24	73.37 ± 18.44	46.65 ± 8.7	0.831, 0.48	126.37 ± 5.03
	SAR	466.19 ± 105.48	673.96 ± 120.51	684.21		767.56 ± 118.16

	Hippocampus			Striatum			
	LI-rTMS	Fo8-rTMS	F, *p*	Sham	LI-rTMS	Fo8-rTMS	F, *p*
Essential AA	96.55 ± 24.03	50.47 ± 25.4	0.944, 0.457	100.36 ± 20.25	61.34 ± 7.75	72.51 ± 39.13	1.378, 0.358
	272.91 ± 44.35	169.84 ± 22.98	2.514, 0.157	141.16 ± 9	171.9 ± 11.3	146.22 ± 9.33	2.194, 0.191
	813.6 ± 214.21	387.37 ± 68.43	2.678, 0.268	443.66 ± 22.42	423.76 ± 43.68	362.24 ± 29.88	2.180, 0.185
	153.39 ± 28.24	83.76 ± 16.85	2.3, 0.164	105.27 ± 6.84	92.49 ± 10.37	88.87 ± 15.37	0.742, 0.514
	60.92 ± 18.99	53.08 ± 29.35	0.228, 0.802	64.16 ± 5.94	46.11 ± 3.2	52.83 ± 25.63	3.195, 0.120
	147.93 ± 19.62	94.47 ± 15.21	2.642, 0.156	14.17 ± 2.41	9.93 ± 2.09	16.05 ± 8.56	0.503, 0.636
	17.51 ± 4.07	12.02 ± 4.27	0.492, 0.634	14.17 ± 2.41	9.93 ± 2.09	16.05 ± 8.56	0.871, 0.479
	287.49 ± 56.22	150.24 ± 27.63	2.498, 0.154	357.31 ± 26.98 †	344.31 ± 23.44 †	237.88 ± 17.71	9.236, 0.010 **
	473.12 ± 64.39	300.34 ± 45.83	2.202, 0.174	234.89 ± 12.31	279.22 ± 25.25	226.13 ± 11.1	1.693, 0.250

(*continued on next page*)

Table 5 (*continued*)

	Hippocampus			Striatum			
	LI-rTMS	Fo8-rTMS	F, *p*	Sham	LI-rTMS	Fo8-rTMS	F, *p*
Non-essential AA	2868.61 ± 559.17	1584.78 ± 242.47	2.064, 0.195	1443.99 ± 137.57	1581.6 ± 172.6	1172.03 ± 95.99	2.509, 0.148
				59.34 ± 11.32		101.49	
	6096.56 ± 1527.88	2698.81 ± 414.42	2.432, 0.165	9892.49 ± 397.31 ††	9312.84 ± 582.58 †	5967.38 ± 676.57	11.539, 0.007 **
	732.6 ± 153.72	488.08 ± 94.45	1.798, 0.233	558.83 ± 45.68	635.88 ± 39.34	503.7 ± 57.81	1.806, 0.234
	13.85 ± 6.11	14.81 ± 4.38	0.336, 0.74	37.34 ± 7.42	18.46 ± 9.21	37.21 ± 11.22	1.312, 0.329
	10839.03 ± 2362.59	5799.36 ± 1181.27	1.753, 0.237	8877.72 ± 575.3	7512.75 ± 257.63	6437.86 ± 728.85	3.394, 0.107
	10303.06 ± 1995.15	6349.81 ± 1191.34	1.334, 0.317	11353.83 ± 534.33	12777.1 ± 1039.23	9713.28 ± 1362.82	1.476, 0.302
	23469.53 ± 3110.99	15958.12 ± 2301.56	1.974, 0.201	21928.97 ± 450.41 †	23762.08 ± 1525.83 †	16322.48 ± 968.73	13.779, 0.006 **
	3133.65 ± 683.14	1596.5 ± 208.84	2.187, 0.185	2981.54 ± 261.22	2671.17 ± 206.58	2229.03 ± 218.24	2.350, 0.163
	1313.05 ± 190.87	728.46 ± 135.31	3.031, 0.106	1407.02 ± 104.91	1483.4 ± 152.33	1046.11 ± 79.48	5.012, 0.043 *
	194.8 ± 55.71	97.39 ± 27.81	1.112, 0.383	199.02 ± 27.68	145.98 ± 11.64	145.38 ± 38.53	1.411, 0.319
		42.12		20.74 ± 6.48		55.75 ± 39.65	0.759, 0.537
Other AA	107.64 ± 10.4 †	50.84 ± 11.73	6.539, 0.027 *	71.35 ± 2.61	64.53 ± 8.46	51.09 ± 8.38	2.432, 0.199
	4013.09 ± 804.78	2218.27 ± 408.65	1.858, 0.221	3093.54 ± 169.64	2745.19 ± 96.09	2313.7 ± 203.44	3.925, 0.079
	4014.57 ± 804.95	2219.3 ± 409.08	1.818, 0.226	3094.25 ± 169.58	2746.38 ± 96.8	2315.51 ± 202.98	3.926, 0.079
	998.19 ± 147.02	781.24 ± 156.8	0.607, 0.57	409.77 ± 50.85	602.67 ± 40.49	450.4 ± 79.91	4.357, 0.063
	140.13 ± 14.86	98.47 ± 14.51	2.014, 0.21	72.07 ± 5.25	98.41 ± 7.34	70.66 ± 6.8	4.638, 0.052
	1140.62 ± 188.97	656.92 ± 95.72	2.399, 0.155	571.78 ± 32.71 ††	461.06 ± 123.46	225.75 ± 41.55	18.784, 0.005 **

F, *p* = F-statistic, *p*-value; Welch's ANOVA, $^{*}p < 0.05$, $^{**}p < 0.01$. *Post hoc* Games-Howell test $^{\dagger}p < 0.05$, $^{\dagger\dagger}p < 0.01$ vs. Fo8-rTMS.
Not included: APA, DA, TPR, GPR, 1MHIS.

stimulation, whereas the second study (Keck et al., 2002) detected significant increases only at a delayed interval after the start of rTMS: 90 min for hippocampus and 30 min for the nucleus accumbens of the striatum (as determined using stereotactic co-ordinates). These differences could be attributed to sampling method (e.g., brain homogenate vs. dialysis and size of dissected tissue), which is discussed in Section 4.2.1.

In addition, variation in the stimulation parameters used such as the magnetic field intensity and shape, frequency and number of pulses delivered could contribute to the different effects of rTMS on the dopaminergic system. Coils used in other studies can induce magnetic field intensities approximately 2–3 times higher than those used in the present study, (i.e., 2.3–4 T), although the absolute intensity was often not provided in these studies; rather, they report stimulation intensity as % stimulator output or % motor threshold, making it difficult to compare methodology. In addition, frequency is suggested to be a key determinant of rTMS outcomes (Wilson and St George, 2016). In the present study, we used a 10 Hz stimulation protocol, whereas others have utilised 20–25 Hz protocols (Ben-Shachar et al., 1997; Kanno et al., 2004; Keck et al., 2002). A statistical regression analysis (i.e., Principal Component Analysis) of rTMS studies has shown that the number and amplitude of the pulses delivered have a weak relationship to motor evoked potentials, a common outcome measure of rTMS (Wilson and St George, 2016).

Overall, the differences between the results of present and previous studies on DA and its metabolites following high intensity rTMS indicate that stimulation parameters such as coil shape, intensity, frequency, pulse number, may differentially regulate various aspects of DA synthesis, binding, release and reuptake. It is, however, uncertain whether the serotonergic system is less sensitive to differences rTMS parameters, as our results are more consistent with previous results. Future studies could investigate the impact of each rTMS parameter, for example changing only the intensity, frequency and pulse number, on the serotonergic and dopaminergic systems.

4.1.2. Other metabolites

Fo8-rTMS also reduced levels of amino acids involved in glutamatergic neurotransmission in the striatum, consistent with the suggestion that alterations to the excitation and inhibition balance within cortical networks are a mechanism of rTMS-induced plasticity (Cirillo et al., 2017; Pell et al., 2011). Similar to GLU, serine and aspartate are excitatory AAs that are necessary for NMDA receptor activation and D-serine can act at the glycine site of the NMDA receptor as a coactivator (D'Ascenzo et al., 2014; Wolosker, 2006). Note here that the observed changes in serine and glutamate concentrations by Fo8-rTMS may be influenced not only by neuronal but also by glial cell function. Although the mechanisms of action are debated, astrocytes are involved in the homeostatic regulation of numerous neuroactive substances including D-serine (Henneberger et al., 2010; Wolosker, 2006; Wolosker et al., 2016), glycine and glutamate (Schousboe, 2019). Interestingly, sarcosine, a precursor AA for the synthesis of glycine, was significantly reduced, although there were no significant changes in glycine concentrations. In addition, threonine was significantly reduced following rTMS, and is a precursor AA for the synthesis of various proteins. This suggests that various metabolic pathways may have been rapidly activated by rTMS, and future studies using methods such as untargeted metabolomics will be useful for characterising changes in the whole metabolic profile of various brain regions.

By contrast, within the hippocampus, only α-aminoadipic acid concentration was regulated by rTMS. α -aminoadipic acid is an inhibitor of kynurenic acid synthesis (Wu et al., 1995) and is gliotoxic (Huck et al., 1984). Kynurenic acid is relevant to synaptic plasticity as it is a relatively non-specific excitatory AA receptor antagonist that is produced endogenously (Ganong et al., 1983) and binds to the glycine site on the NMDA receptor (Stone, 1993). Bath application of kynurenic acid has been shown to antagonise hippocampal excitatory postsynaptic

potentials (Ganong et al., 1983). Thus, the reduction of α-aminoadipic acid observed in the hippocampus of Fo8-rTMS animals may result in decreased excitatory activity within the hippocampus. Future studies could investigate the relationship between α-aminoadipic acid and kynurenic acid pathways following rTMS to elucidate the underlying mechanisms.

4.1.3. Comparison with human studies

Analysis of neurotransmitter levels following rTMS in humans has not been extensively performed. For 5-HT levels, long term studies have been carried out in patients with depression: following daily 10 Hz rTMS at 110% motor threshold for two weeks, 5-HT binding in the prefrontal cortex was increased and positively correlated with improvement in Hamilton Rating Scale for Depression scale but binding in the hippocampus decreased and was negatively correlated with outcomes (Baeken et al., 2011). Using [11C] raclopride binding and positron emission tomography, Strafella et al. (2003) showed that rTMS of the prefrontal cortex induces the release of endogenous DA in the ipsilateral caudate nucleus in healthy participants, consistent with our finding of neurotransmitter changes distant from the site of direct stimulation (i.e., subcortical changes following rTMS).

4.1.3.1. Cortical vs subcortical regions. In the present study, cortical DA concentrations were unaltered following Fo8-rTMS, although we observed a reduction in 5-HT turnover rates. We speculate that the different results may be due to the unique patterns of DA and 5-HT innervation of the cortex. Dopaminergic innervation of the cortex is sparse and heterogenous as compared to the widespread projections of serotonergic neurons (Berger et al., 1991). Therefore, it is possible that any regional rTMS-induced effects on DA concentrations were masked by our sampling of the entire cortex. In addition, specific regions within the cortex may be differentially susceptible to the effects of rTMS, as suggested by the heterogenous protein expression of the immediate early gene *zif*268 in the cortex following rTMS (Aydin-Abidin et al., 2008). Future studies could therefore investigate the effect of rTMS in particular cortical regions that have comparable dopaminergic terminal densities to those in primates, such as the prefrontal cortex (Berger et al., 1991). Although regional differences in 5-HT concentrations have also been described in the rodent cortex, albeit at much higher concentrations than that of DA (Reader and Grondin, 1987), our results suggests that high intensity Fo8-rTMS induces widespread changes to the serotonergic system, either through direct stimulation of terminals, or *via* stimulation of intracortical circuits, resulting in the observed reduction in 5-HT turnover rates.

We also found changes in subcortical regions, raising the question of whether these effects, detected remotely from the stimulation site, are due to direct stimulation of regions located deep within the rodent brain, or indirect stimulation of these regions *via* activation of cortical neurons. While it is possible that Fo8-rTMS in our study delivered stimulation to the hippocampus and striatum at an intensity sufficiently high to induce action potentials and alter neurotransmitter and amino acid metabolic pathways, there is evidence from the literature that cortical stimulation is sufficient to activate other brain regions. Comparison of resting brain activity using fMRI has shown alterations to subcortical regions following high intensity rTMS in humans (Bestmann et al., 2004) and LI-rTMS in rats (Seewoo et al., 2018), suggesting that both Fo8-and LI-rTMS are capable of modulating corticofugal connections to regions that are not within direct range of the induced electric field. It is likely that Fo8-rTMS induces action potential firing of corticofugal projecting neurons (Banerjee et al., 2017), thus resulting in the significant changes we observed at the subcortical level.

4.2. Different effects of LI-rTMS and Fo8-rTMS

It was unexpected that LI-rTMS of awake and freely moving animals had no significant effect on any of the compounds investigated in the present study; this is because we previously described, after a single LI-rTMS session, altered resting state activity in rodents *in vivo* (Seewoo et al., 2018), as well changes to gene expression (Grehl et al., 2015) and levels of neurotransmitters and cellular metabolites associated with the Krebs cycle *in vitro* (Hong et al., 2018). It is possible that LI-rTMS-induced changes in neurotransmitter levels *in vivo* may be too subtle to be detected following a single stimulation session, even with our highly sensitive method, and we note that 5-HT and DA levels following LI-rTMS followed similar patterns to those following Fo8-rTMS, but did not reach statistical significance. The lower impact of LI- compared to Fo8-rTMS is consistent with the different mechanisms activated by low and high intensity magnetic fields: high intensity rTMS evokes action potentials, directly triggering neurotransmitter release, whereas LI-rTMS does not induce neuronal firing but rather causes an increase in excitability by reducing action potential threshold and increasing spike firing potential (Tang et al., 2016). As a result, the effects of LI-rTMS on neurotransmitter levels may be more prominent after multiple stimulation sessions, consistent with the significant molecular, structural and functional changes induced by LI-rTMS *in vivo* following chronic treatment (Makowiecki et al., 2014; Poh et al., 2018; Rodger et al., 2012).

However, in addition to delivering different intensities, our LI-rTMS and Fo8-rTMS protocols differed significantly in the parameters of the two stimulation devices. Firstly, the coil that was used for Fo8-rTMS was a large figure-of-eight coil that would have stimulated all of the head and part of the body of the mouse, whereas the small circular coil used for LI-rTMS targeted the brain more focally. These devices further differ from those used in other animal studies, which most commonly used figure-of-eight shaped coils of varying diameter (Aydin-Abidin et al., 2006; Ben-Shachar et al., 1997; El Arfani et al., 2017; Kanno et al., 2004; Keck et al., 2002; Zangen and Hyodo, 2002). It is therefore not possible to conclude that the differences we observe here between LI- and Fo8-rTMS are due solely to the intensity of stimulation. Other parameters such as differences in coil shape and orientation relative to the brain, as well as pulse parameters (see for example: Lu and Ueno, 2017; Opitz et al., 2016) are likely to have contributed to the results of the present study. An approach to specifically investigate the role of intensity would be to reduce the intensity of the Fo8-rTMS to be equivalent to the LI-rTMS coil, however this was not possible as 1% of the MagVenture stimulator output is still an order of magnitude higher than LI-rTMS. The other option, to increase the power supply to the small coils to produce a magnetic field intensity that matched that of Fo8-rTMS, was not physically possible due to overheating of the small coil. We also acknowledge that pulse number and duration of stimulation were limited by the physical properties of the coils (i.e., overheating of the MagVenture coil). Our study is therefore limited to comparing outcomes of two different types of rTMS stimulation that have been used in the animal rTMS literature, without identifying the specific parameters responsible for the differences. Future studies which involve magnetic and electric field modelling, as well as innovative design of miniaturised rTMS devices that enable comparative studies in animal models and human subjects with matching stimulation paradigms will be crucial for dissecting the contributions of different rTMS parameters (Rodger and Sherrard, 2015).

4.2.1. Differences in sampling method

Many studies have assessed concentration changes by sampling brain microdialysates, limitations include a minimum volume of sample required for sampling, which can take up to 10 min per time sample and a high level of technical knowledge and training. In addition, surgical placement of the cannula or probe is relatively large, especially when targeting the extracellular space of specific nuclei within the mouse brain (Shippenberg and Thompson, 2001). Therefore, the benefit of assessing concentration changes using homogenates is the relative ease of sample collection, requiring only good anatomical knowledge and dissection skill. Magnetic stimulation-induced changes to AA

concentrations are not limited to the extracellular space, but also occur intracellularly. Thus, investigating changes to AA concentrations from homogenates may provide a greater overview of the changes occurring within a particular sample, and allow researchers to develop novel biomarkers of the brain in healthy and pathophysiological states. Limitations of this method include the ability to collect samples only at a specific time point (post-mortem), whereas microdialysis and non-invasive imaging techniques allow repeated and longitudinal studies, although they may be less accurate. Therefore, the sampling method selected will depend on the scientific aims and hypotheses of each study.

In the present sampling method, the entire cortex and striatum was dissected. In future, studies could look at dissecting a more specific region, for example directly under the stimulation site in the cortex, the prefrontal cortex and differentiating the dorsal and ventral striatum. In addition, we were unable to quantitate HVA levels in the hippocampus due to low S/N ratios. The presence of DA and the other major metabolite, DOPAC, suggests that it should have been present in the hippocampus. A possible reason for the inability of the present method to detect HVA may be due to the addition of a fixed volume of perchloric acid to dissolve the tissue samples (300 µL), which may have reduced the total HVA content during sampling. Nonetheless, the LC-MS/MS method we have described is extremely sensitive and in the present study, we were able to quantify extremely low concentrations of particular AAs such as threonine (at 0.594 pM). Therefore, future studies could add perchloric acid in a fixed wet weight-to-volume ratio, e.g. 10 µL acid per 1 mg brain tissue. By adopting these methods, future studies can minimise the number of missing values and thus provide a more complete dataset.

4.3. Conclusions

In the present study, we developed a rapid and accurate method in combination with a commercially available kit, with minimal sample preparation, to assay DA, 5-HT and their metabolites (DOPAC, HVA; 5-HIAA) with an intra- and inter-day precision that was below 13%, and 27 different AAs in mouse brain homogenates, with a CV% $<$ 15% for those found to be significantly different. This method will be useful for future studies to characterise and screen for brain biomarkers in both the healthy and diseased state that can be assayed simultaneously in a single run; leading to the development of methods that can target AAs to a high degree of specificity and accuracy, as done for DA, 5-HT and their metabolites in the present study. Our results highlight the importance of gaining a better understanding of how rTMS parameters, including stimulator dimensions, contribute to neurochemical changes throughout the brain, in order to maximise the efficacy of rTMS therapies.

Declarations of interest

None.

Acknowledgements

EZP is supported by an Australian Government Research Training Program scholarship and partially supported by the German Academic Exchange Service (DAAD). JR is a MSWA/Perron Senior Research Fellow. Part of this research was supported by the Neurotrauma Research Program, WA. MWC is affiliated to Metabolomics Australia, UWA, and is supported by infrastructure funding from the Western Australian State Government in partnership with the Australia Federal Government through the National Collaborative Research Infrastructure Strategy (NCRIS).

Appendix A. Supplementary data

Supplementary data to this article can be found online at https://doi.org/10.1016/j.neuint.2019.104546.

References

Aydin-Abidin, S., Moliadze, V., Eysel, U.T., Funke, K., 2006. Effects of repetitive TMS on visually evoked potentials and EEG in the anaesthetized cat: dependence on stimulus frequency and train duration. J. Physiol. 574, 443–455. https://doi.org/10.1113/jphysiol.2006.108464.

Aydin-Abidin, S., Trippe, J., Funke, K., Eysel, U.T., Benali, A., 2008. High- and low-frequency repetitive transcranial magnetic stimulation differentially activates c-Fos and zif268 protein expression in the rat brain. Exp. Brain Res. 188, 249–261. https://doi.org/10.1007/s00221-008-1356-2.

Badgaiyan, R.D., 2014. Imaging dopamine neurotransmission in live human brain. Prog. Brain Res. https://doi.org/10.1016/B978-0-444-63425-2.00007-6.

Baeken, C., De Raedt, R., Bossuyt, A., Van Hove, C., Mertens, J., Dobbeleir, A., Blanckaert, P., Goethals, I., 2011. The impact of HF-rTMS treatment on serotonin(2A) receptors in unipolar melancholic depression. Brain Stimul 4, 104–111. https://doi.org/10.1016/j.brs.2010.09.002.

Banerjee, J., Sorrell, M.E., Celnik, P.A., Pelled, G., 2017. Immediate effects of repetitive magnetic stimulation on single cortical pyramidal neurons. PLoS One. https://doi.org/10.1371/journal.pone.0170528.

Barton, D.A., Esler, M.D., Dawood, T., Lambert, E.A., Haikerwal, D., Brenchley, C., Socratous, F., Hastings, J., Guo, L., Wiesner, G., Kaye, D.M., Bayles, R., Schlaich, M.P., Lambert, G.W., 2008. Elevated brain serotonin turnover in patients with depression: effect of genotype and therapy. Arch. Gen. Psychiatr. https://doi.org/10.1001/archgenpsychiatry.2007.11.

Ben-Shachar, D., Belmaker, R.H., Grisaru, N., Klein, E., 1997. Transcranial magnetic stimulation induces alterations in brain monoamines. J. Neural Transm. 104, 191–197.

Berger, B., Gaspar, P., Verney, C., 1991. Dopaminergic innervation of the cerebral cortex: unexpected differences between rodents and primates. Trends Neurosci. https://doi.org/10.1016/0166-2236(91)90179-X.

Bestmann, S., Baudewig, J., Siebner, H.R., Rothwell, J.C., Frahm, J., 2004. Functional MRI of the immediate impact of transcranial magnetic stimulation on cortical and subcortical motor circuits. Eur. J. Neurosci. 19, 1950–1962. https://doi.org/10.1111/j.1460-9568.2004.03277.x.

Carmi, L., Alyagon, U., Barnea-Ygael, N., Zohar, J., Dar, R., Zangen, A., 2018. Clinical and electrophysiological outcomes of deep TMS over the medial prefrontal and anterior cingulate cortices in OCD patients. Brain Stimul. https://doi.org/10.1016/j.brs.2017.09.004.

Cirillo, G., Di Pino, G., Capone, F., Ranieri, F., Florio, L., Todisco, V., Tedeschi, G., Funke, K., Di Lazzaro, V., 2017. Neurobiological after-effects of non-invasive brain stimulation. Brain Stimul. https://doi.org/10.1016/j.brs.2016.11.009.

D'Ascenzo, M., Podda, M.V., Grassi, C., 2014. The role of D-serine as co-agonist of NMDA receptors in the nucleus accumbens: relevance to cocaine addiction. Front. Synaptic Neurosci. https://doi.org/10.3389/fnsyn.2014.00016.

El Arfani, A., Parthoens, J., Demuyser, T., Servaes, S., De Coninck, M., De Deyn, P.P., Van Dam, D., Wyckhuys, T., Baeken, C., Smolders, I., 2017. Accelerated high-frequency repetitive transcranial magnetic stimulation enhances motor activity in rats. Neuroscience.

Ewles, M., Goodwin, L., 2011. Bioanalytical approaches to analyzing peptides and proteins by LC–MS/MS. Bioanalysis 3, 1379–1397. https://doi.org/10.4155/bio.11.112.

Ganong, A.H., Lanthorn, T.H., Cotman, C.W., 1983. Kynurenic acid inhibits synaptic and acidic amino acid-induced responses in the rat hippocampus and spinal cord. Brain Res. https://doi.org/10.1016/0006-8993(83)91108-3.

Grace, A.A., 2004. Developmental dysregulation of the dopamine system and the pathophysiology of schizophrenia. Neurodev. Schizophr. 273–294. https://doi.org/10.1038/nrn.2016.57.

Grehl, S., Viola, H.M., Fuller-Carter, P.I., Carter, K.W., Dunlop, S.A., Hool, L.C., Sherrard, R.M., Rodger, J., 2015. Cellular and molecular changes to cortical neurons following low intensity repetitive magnetic stimulation at different frequencies. Brain Stimul 8, 114–123. https://doi.org/10.1016/j.brs.2014.09.012.

Heath, A., Lindberg, D.R., Makowiecki, K., Gray, A., Asp, A.J., Rodger, J., Choi, D.S., Croarkin, P.E., 2018. Medium- and high-intensity rTMS reduces psychomotor agitation with distinct neurobiologic mechanisms. Transl. Psychiatry. https://doi.org/10.1038/s41398-018-0129-3.

Henneberger, C., Papouin, T., Oliet, S.H.R., Rusakov, D.A., 2010. Long-term potentiation depends on release of d-serine from astrocytes. Nature. https://doi.org/10.1038/nature08673.

Hilbert, S., McAssey, M., Bühner, M., Schwaferts, P., Gruber, M., Goerigk, S., Taylor, P.C.J., 2019. Right hemisphere occipital rTMS impairs working memory in visualizers but not in verbalizers. Sci. Rep. https://doi.org/10.1038/s41598-019-42733-6.

Hong, I., Garrett, A., Maker, G., Mullaney, I., Rodger, J., Etherington, S.J., 2018. Repetitive low intensity magnetic field stimulation in a neuronal cell line: a metabolomics study. PeerJ. https://doi.org/10.7717/peerj.4501.

Huck, S., Grass, F., Hatten, M.E., 1984. Gliotoxic effects of α-aminoadipic acid on monolayer cultures of dissociated postnatal mouse cerebellum. Neuroscience. https://doi.org/10.1016/0306-4522(84)90170-2.

Kanno, M., Matsumoto, M., Togashi, H., Yoshioka, M., Mano, Y., 2004. Effects of acute repetitive transcranial magnetic stimulation on dopamine release in the rat dorsolateral striatum. J. Neurol. Sci. 217, 73–81. https://doi.org/10.1016/j.jns.2003.08.

013.
Keck, M.E., Welt, T., Muller, M.B., Erhardt, A., Ohl, F., Toschi, N., Holsboer, F., Sillaber, I., 2002. Repetitive transcranial magnetic stimulation increases the release of dopamine in the mesolimbic and mesostriatal system. Neuropharmacology 43, 101–109. ([pii]). https://doi.org/10.1016/s0028-3908(02)00069-2.
Kim, M., Lee, J. gyeom, Yang, C.H., Lee, S., 2016. Silica stationary phase-based on-line sample enrichment coupled with LC-MS/MS for the quantification of dopamine, serotonin and their metabolites in rat brain microdialysates. Anal. Chim. Acta. https://doi.org/10.1016/j.aca.2016.03.021.
Lefaucheur, J.-P., André-Obadia, N., Antal, A., Ayache, S.S., Baeken, C., Benninger, D.H., Cantello, R.M., Cincotta, M., de Carvalho, M., De Ridder, D., 2014. Evidence-based guidelines on the therapeutic use of repetitive transcranial magnetic stimulation (rTMS). Clin. Neurophysiol. 125, 2150–2206.
Leonhardt, J., Teutenberg, T., Tuerk, J., Schlüsener, M.P., Ternes, T.a., Schmidt, T.C., 2015. A comparison of one-dimensional and microscale two-dimensional liquid chromatographic approaches coupled to high resolution mass spectrometry for the analysis of complex samples. Anal. Methods. https://doi.org/10.1039/C5AY01143D.
Lu, M., Ueno, S., 2017. Comparison of the induced fields using different coil configurations during deep transcranial magnetic stimulation. PLoS One. https://doi.org/10.1371/journal.pone.0178422.
Makowiecki, K., Harvey, A.R., Sherrard, R.M., Rodger, J., 2014. Low-intensity repetitive transcranial magnetic stimulation improves abnormal visual cortical circuit topography and upregulates BDNF in mice. J. Neurosci. 34, 10780–10792. https://doi.org/10.1523/JNEUROSCI.0723-14.2014.
Meiser, J., Weindl, D., Hiller, K., 2013. Complexity of dopamine metabolism. Cell Commun. Signal. https://doi.org/10.1186/1478-811X-11-34.
Michael, N., Gösling, M., Reutemann, M., Kersting, A., Heindel, W., Arolt, V., Pfleiderer, B., 2003. Metabolic changes after repetitive transcranial magnetic stimulation (rTMS) of the left prefrontal cortex: a sham-controlled proton magnetic resonance spectroscopy (1H MRS) study of healthy brain. Eur. J. Neurosci. https://doi.org/10.1046/j.1460-9568.2003.02683.x.
Myhrer, T., 2003. Neurotransmitter systems involved in learning and memory in the rat: a meta-analysis based on studies of four behavioral tasks. Brain Res. Rev. https://doi.org/10.1016/S0165-0173(02)00268-0.
Opitz, A., Fox, M.D., Craddock, R.C., Colcombe, S., Milham, M.P., 2016. An integrated framework for targeting functional networks via transcranial magnetic stimulation. Neuroimage. https://doi.org/10.1016/j.neuroimage.2015.11.040.
O'Reardon, J.P., Cristancho, P., Pilania, P., Bapatla, K.B., Chuai, S., Peshek, A.D., 2007a. Patients with a major depressive episode responding to treatment with repetitive transcranial magnetic stimulation (rTMS) are resistant to the effects of rapid tryptophan depletion. Depress. Anxiety 24, 537–544. https://doi.org/10.1002/da.20261.
O'Reardon, J.P., Solvason, H.B., Janicak, P.G., Sampson, S., Isenberg, K.E., Nahas, Z., McDonald, W.M., Avery, D., Fitzgerald, P.B., Loo, C., Demitrack, M.A., George, M.S., Sackeim, H.A., 2007b. Efficacy and safety of transcranial magnetic stimulation in the acute treatment of major depression: a multisite randomized controlled trial. Biol. Psychiatry 62, 1208–1216. https://doi.org/10.1016/j.biopsych.2007.01.018.
Pell, G.S., Roth, Y., Zangen, A., 2011. Modulation of cortical excitability induced by repetitive transcranial magnetic stimulation: influence of timing and geometrical parameters and underlying mechanisms. Prog. Neurobiol. 93, 59–98. https://doi.org/10.1016/j.pneurobio.2010.10.003.
Poh, E.Z., Harvey, A.R., Makowiecki, K., Rodger, J., 2018. Online LI-rTMS during a visual learning task: differential impacts on visual circuit and behavioural plasticity in adult Ephrin-A2A5-/- mice. eNeuro. https://doi.org/10.1523/ENEURO.0163-17.2018.
Reader, T.A., Grondin, L., 1987. Distribution of catecholamines, serotonin, and their major metabolites in the rat cingulate, piriform-entorhinal, somatosensory, and visual cortex: a biochemical survey using high-performance liquid chromatography. Neurochem. Res. https://doi.org/10.1007/BF00971709.
Rodger, J., Sherrard, R.M., 2015. Optimising repetitive transcranial magnetic stimulation for neural circuit repair following traumatic brain injury. Neural Regen. Res. 10, 357.
Rodger, J., Mo, C., Wilks, T., Dunlop, S.A., Sherrard, R.M., 2012. Transcranial pulsed magnetic field stimulation facilitates reorganization of abnormal neural circuits and corrects behavioral deficits without disrupting normal connectivity. FASEB J. 26, 1593–1606. https://doi.org/10.1096/fj.11-194878.
Schousboe, A., 2019. Metabolic signaling in the brain and the role of astrocytes in control of glutamate and GABA neurotransmission. Neurosci. Lett. 689, 11–13. https://doi.org/10.1016/J.NEULET.2018.01.038.
Seewoo, B.J., Feindel, K.W., Etherington, S.J., Rodger, J., 2018. Resting-state fMRI study of brain activation using low-intensity repetitive transcranial magnetic stimulation in rats. Sci. Rep. https://doi.org/10.1038/s41598-018-24951-6.
Shippenberg, T.S., Thompson, A.C., 2001. Overview of microdialysis. Curr. Protoc. Neurosci. https://doi.org/10.1002/0471142301.ns0701s00.
Stone, T.W., 1993. Neuropharmacology of quinolinic and kynurenic acids. Pharmacol. Rev.
Strafella, A.P., Paus, T., Barrett, J., Dagher, A., 2001. Repetitive transcranial magnetic stimulation of the human prefrontal cortex induces dopamine release in the caudate nucleus. J. Neurosci. 21, 1–4. ([pii]). https://doi.org/10.1523/jneurosci.21-15-j0003.2001.
Strafella, A.P., Paus, T., Fraraccio, M., Dagher, A., 2003. Striatal dopamine release induced by repetitive transcranial magnetic stimulation of the human motor cortex. Brain 126, 2609–2615. https://doi.org/10.1093/brain/awg268.
Tang, A., Thickbroom, G., Rodger, J., 2015. Repetitive transcranial magnetic stimulation of the brain mechanisms from animal and experimental models. Neuroscience 1073858415618897. https://doi.org/10.1177/1073858415618897.
Tang, A.D., Hong, I., Boddington, L.J., Garrett, A.R., Etherington, S., Reynolds, J.N., Rodger, J., 2016. Low-intensity repetitive magnetic stimulation lowers action potential threshold and increases spike firing in layer 5 pyramidal neurons in vitro. Neuroscience 335, 64–71. https://doi.org/10.1016/j.neuroscience.2016.08.030.
Thomas, M.J., Kalivas, P.W., Shaham, Y., 2008. Neuroplasticity in the mesolimbic dopamine system and cocaine addiction. Br. J. Pharmacol. https://doi.org/10.1038/bjp.2008.77.
Vahabzadeh-Hagh, A.M., Muller, P.A., Gersner, R., Zangen, A., Rotenberg, A., 2012. Translational neuromodulation: approximating human transcranial magnetic stimulation protocols in rats. Neuromodulation. https://doi.org/10.1111/j.1525-1403.2012.00482.x.
Verma, A., Kumar, I., Verma, N., Aggarwal, P., Ojha, R., 2016. Magnetic resonance spectroscopy - revisiting the biochemical and molecular milieu of brain tumors. BBA Clin. https://doi.org/10.1016/j.bbacli.2016.04.002.
Wilson, M.T., St George, L., 2016. Repetitive transcranial magnetic stimulation: a call for better data. Front. Neural Circuits.
Winograd-Gurvich, C., Fitzgerald, P.B., Georgiou-Karistianis, N., Bradshaw, J.L., White, O.B., 2006. Negative symptoms: a review of schizophrenia, melancholic depression and Parkinson's disease. Brain Res. Bull. 70, 312–321. https://doi.org/10.1016/j.brainresbull.2006.06.007.
Wolosker, H., 2006. D-serine regulation of NMDA receptor activity. Sci. STKE. https://doi.org/10.1126/stke.3562006pe41.
Wolosker, H., Balu, D.T., Coyle, J.T., 2016. The rise and fall of the D-serine-mediated gliotransmission hypothesis. Trends Neurosci. https://doi.org/10.1016/j.tins.2016.09.007.
Wu, H.Q., Ungerstedt, U., Schwarcz, R., 1995. l-α-Aminoadipic acid as a regulator of kynurenic acid production in the hippocampus: a microdialysis study in freely moving rats. Eur. J. Pharmacol. https://doi.org/10.1016/0014-2999(95)00224-9.
Zimmermann, M., Verhagen, L., de Lange, F.P., Toni, I., 2016. The extrastriate body area computes desired goal states during action planning. eNeuro. https://doi.org/10.1523/ENEURO.0020-16.2016.
Zangen, A., Hyodo, K., 2002. Transcranial magnetic stimulation induces increases in extracellular levels of dopamine and glutamate in the nucleus accumbens. Neuroreport. https://doi.org/10.1097/01.wnr.0000048021.74602.f2.